OSA Latin America Optics & Photonics Conference

12–15 November 2018

Pontificia Universidad Católica del Perú, Lima, Peru

Table of Contents

Th4A • Poster Session II—Continued

Th4A.25
Optical Demonstration of a Programmable Multi-channel Polarization Beamsplitter, Dudbil Pabon[1,2], Sebastian Bordaquevich[1], Claudio Iemmi[1,2], Lorena Rebón[3], Silvia A. Ledesma[1,2]; *[1]Laboratorio de Procesado de Imágenes, Departamento de Física , Facultad de Ciencias Exactas y Naturales, Universidad de Buenos Aires, Argentina; [2]CONICET, Argentina; [3]Instituto de Física de La Plata - UNLP – CONICET, Argentina.* We present a method that allows us to obtain different polarizations in different directions of the space acting as a multi-channel beamsplitter using a spatial light modulator (SLM) with different gray levels.

Th4A.26
Determination of Any Pure Spatial Qudit from 4d −3 Projective Measurements, Quimey Pears Stefano[1,2], Lorena Rebón[3], Silvia A. Ledesma[1,2], Claudio Iemmi[1,2]; *[1]Laboratorio de Procesado de Imágenes, Departamento de Física , Facultad de Ciencias Exactas y Naturales, Universidad de Buenos Aires, Argentina; [2]CONICET, Argentina; [3]Departamento de Física, Instituto de Física de La Plata - UNLP – CONICET, Argentina.* We present a quantum tomography method that allows to characterize any pure qudit of arbitrary dimension d, with only 4d − 3 proyective measurements. We verified the feasibility of the method with numerical simulations that include the effect of Poissonian detection noise.

Th4A.27
Nonparaxial Electromagnetic Bragg Scattering in Periodic Media with PT Symmetry, Solange B. Cavalcanti[1], Paulo A. Brandão[1], José Henrique Nascimento[1]; *[1]Universidade Federal de Alagoas, Brazil.* Resonant Bragg modes evolution through a PT-symmetric photonic lattice is investigated. Non-paraxial wave solutions lead to nonreciprocal and unidirectional energy exchange between the pair in all regimes defined by the symmetry breaking point.

Th4A.28
A Simple Method for Characterizing the Dispersion of Epsilon-Near Zero Materials, Vinicius T. Alvarenga[1], Christiano José de Matos[1]; *[1]MackGraphe, Mackenzie Presbyterian Univ., Brazil.* We determine the dielectric function spectrum of a material in the 0-1 range, by analyzing the reflectance spectrum as a function of incidence angle. Results obtained for silicon carbide closely match data from the literature.

Th4A.29
Eclipse Intensity Scan Technique, Vinicius Ferreira[1], Ricardo Correia[1]; *[1]Univ Federal do Rio Grande do Sul, Brazil.* We present an eclipsed setup to improve the sensitivity and signal noise ratio of the I-scan technique. We demonstrate here that EI-scan is able to characterize nonlinear optical properties with good sensibility of inomogeneous samples.

Th4A.30
Scatter Search Applied to the Taper Optimization, Luana da França Vieira[1], Vitaly F. Rodriguez Esquerre[1], Anderson Dourado Sisnando[2], Cosme Eustaquio Rubio Mercedes[3]; *[1]DEE UFBA, Brazil; [2]UFRB, Brazil; [3]UEMS, Brazil.* We report the implementation of an algorithm based on the Scatter Search (SS) together with the Finite Element Method (FEM) for the optimization of waveguide couplers between a continuous waveguide (CWG) and a periodically segmented waveguide (PSW).

Th4A.31
Sensors Based on Metamaterial Cladded Waveguides, Juarez Caetano da Silva[2], Vitaly F. Rodriguez Esquerre[1]; *[1]DEE UFBA, Brazil; [2]IFBA, Brazil.* We propose and analyze a sensor based on cladded metamaterial waveguides for monitoring gas or liquid specimens. These structures are made of metal and dielectric thin layers claddings, surrounding the hollow core of the sensor. The sensor sensitivity to the optical response of the samples in the core was obtained to every architecture simulated.

Th4A.32
Analysis of Fibonacci Hypercrystal Metamaterials , Miriele Carvalho Paim[1], Joaquim Junior Isidio de Lima[2], Vitaly F. Rodriguez Esquerre[1]; *[1]DEE UFBA, Brazil; [2]UNIVASF, Brazil.* In this article the properties of a photonic hypercrystal has been analyzed. The structure consists of pairs of metal-dielectric layers separated by air following a Fibonacci sequence. We have demonstratedasymmetrical optical properties that enable the behavior as band mirrors, filters or absorbers for visible and infrared radiation.

Th4A.33
Effect of the High Intensity Laser Nd:YAG in Patients with Vascular Malformations Submitted to Photocoagulation at Brazilian School of Dentistry, Wilber E. Bernaola Paredes[1,2]; *[1]Stomatology, Hospital A. C. Camargo Cancer Center, Brazil; [2]Oral Diagnosis and Stomatology, School of Dentistry, Univ. of São Paulo, Brazil.* The aim of this study was to assess the effectiveness of Nd: YAG laser photocoagulation in the treatment of vascular malformations in the oral and perioral area in Clinical attendace of Oral Medicine at Brazilian center.

Th4A.34
Characterization of UV-induced Absorption and Scattering Losses in Photosensitive Fibers, Xavier Roselló-Mechó[1], Martina Delgado-Pinar[1], José L. Cruz[1], Antonio Diez[1], Miguel V. Andrés[1]; *[1]Universitat de València, Spain.* We present a technique to measure the absorption coefficient increment induced during the UV-inscription of gratings in photosensitive fibers. Our technique also allows discriminating between the absorption and scattering contributions to the overall losses.

Th4A.35
Development of a Wide Range Hyperspectral Imager for Evidence Examination, Xuejun Zhao[1,2], Nengbin Cai[3,2], Shan He[1,2], Xiaochun Huang[3,2], Wenbin Liu[1,2], Huaimiao Hua[3,2], Jiyun Zhang[3,2]; *[1]Shanghai Research Inst. of Criminal Science and Technology, China; [2]Shanghai Key Laboratory of Crime Scene Evidence, China; [3]Shanghai Inst. of Forensic Science, Public Security Bureau, China.* By adjusting the attitude, frame rate and moving speed of two hyperspectral imager, the matching method of line-of-sight field of the two equipments was studied, and the wide range imaging from 400 nm to 1700 nm was realized.

Th4A.36
Modelling of Structural and Material Parameters of Optical Planar Waveguide to Control Birefringence, Yaman Parasher[1], Akshay Kaushik[2], Gurjit Kaur[3], Prabhot Singh[4]; *[1]Electronics and Communication, Gautam Buddha Univ., India; [2]Electronics and Communication, Sanskar College of Engineering and Technology, India; [3]Electronics and Communication, Delhi Technological Univ., India; [4]Salesforce.com EMEA Ltd, San Francisco, CA, USA, USA.* Birefringence is observed when layers in the optical planar waveguide exhibits stresses at elevated temperature. To design birefringence free waveguide structure, we carefully modelled the structural, material parameters with the help of a thermal stress formula.

Th4A.37
Features of Narrow-band ASE Noise Pulsing, Yuri O. Barmenkov[1], Pablo Muniz-Cánovas[1], Alexander V. Kir'yanov[1], Jose L. Cruz[2], Miguel V. Andrés[2]; *[1]Centro de Investigaciones en Optica AC, Mexico; [2]Universidad de Valencia, Spain.* The results of an experimental study of noise features of polarized and unpolarized amplified spontaneous emission (ASE) with narrow optical bandwidth, registered from standard low-doped erbium fiber pumped at 976 nm, are presented.

Th4A.38
Picosecond Non-Radiative Relaxation in Indole Studied by Interferometric Pump-Probe Method, Alexey Glazov[1], Alexander Sukharev[1], Irina Semenova[1], Oleg Vasyutinskii[1]; *[1]Ioffe Inst., Russian Federation.* A new interferometric pump-probe method based on the detection of local refractive index is proposed and used for studing non-radiative lifetime of high-laying vibronic energy states in indole dissolved in propylene glycol and two-photon excited by femtosecond laser pulses at 400 nm. The lifetime of the exited states and found to be below 40 ps.

Th4A.39
New Optical Approach to Simultaneous Determination of Deformability and Adhesion Energy of Human Erythrocytes, Bibiana D. Riquelme[1,2], Carolina Londero[1,2]; *[1]Fac Cs. Bioquimicas y Farmaceuticas. UNR, Argentina; [2]Instituto de Física Rosario (CONICET-UNR), Argentina.* We present an optical microfluidic device that allows the simultaneous determination of deformability and energy adhesion parameters of erythrocytes applying the new optical technologies for acquisition and image analysis using an inverted optical microscope.

Th4A.40
Photonics Techniques Applied to the Characterization of Polyamidoamine (PAMAM) Dendrimers to be Employed as Drug Delivery System (DDS), David Ybarra[1], Daniela Igartúa[1], Maria Eugenia Tuttolomondo[3], Silvia del Valle Alonso[1], Fernando C. Alvira[1,2]; *[1]Laboratorio de Biomembranas, Universidad Nacional de Quilmes, Argentina; [2]Laboratorio de Instrumentacion, Automatizacion y Control, Universidad Nacional de Quilmes, Argentina; [3]Cátedra de Fisicoquímica I, INQUINOA, Argentina.* We have characterized PAMAM dendrimers by Raman and UV-VIS spectroscopy. Those experiments showed the spectroscopic behavior of dendrimer chemical groups at different pH. This will help to a better understanding of drug-dendrimer interactions.

Th4A.41
Linear and Non-linear Viscoelasticity of Red Blood Cells Using a New Optical Erythrocyte Rheometer, Bibiana D. Riquelme[1,2], Horacio Castellini[3], Brenda Albea[1]; *[1]Fac Cs. Bioquimicas y Farmaceuticas. UNR, Argentina; [2]Instituto de Física Rosario (CONICET-UNR), Argentina; [3]Fac. Cs. Exactas, Ingeniería y Agrimensura (UNR), Argentina.* Linear and non-linear viscoelasticity of red blood cells was characterized using a new Optical Erythrocyte Rheometer based on laser diffractometry technique. Optical and mechanical models were developed to obtain representative parameters for clinical application.

Th4A.42
FTIR spectroscopy: an optical method to study wound healing process, Pedro A. Castro[2], Cássio Lima[2], Telma T. Zorn[1], Denise M. Zezell[2]; *[1]ICB, Univ. of Sao Paulo, Brazil; [2]IPEN-CNEN/SP, Univ. of Sao Paulo, Brazil.* In this study, we investigated the ability of Fourier transform infrared spectroscopy to discriminate healthy tissue and thermal injury, aiming the development of an optical method to evaluate the wound healing process.

Th4A.43
Coupling Length of a Non-symmetric Directional Coupler Implemented in a Microstructured Optical Fiber, Sergei Khotiaintsev[1], María del Carmen Lopez-Bautista[1], Alexander Martynyuk[1]; *[1]Telecommunications, National Autonomus Univ. of Mexico, Mexico.* We analyzed the effect of some geometrical parameters on the coupling length of a special non-symmetric optical directional coupler employed as a low-refractive-index sensor. Our results can help to choose the realistic length of the coupler.

Th4A.44
Growth and Post-processing Effects of Graphene through Hyperspectral X-ray Absorption Spectroscopy: Theory, Experiment and Data, Wudmir Y. Rojas[1], Allen Winter[1], Daniel Fischer[2], Edward Principe[3], Chuong Hynh[4], Sarbajit Banerjee[5], David Prendergast[6], Apurva Mehta[7], James Grote[8], Eva Campo[1]; *[1]Bangor Univ., UK; [2]National Inst. of Standards and Technology, USA; [3]Synchrotron Research Inc., USA; [4]Carl Zeiss Microscopy, LLC, One Corporation Way, USA; [5]Department of Chemistry, Texas A&M Univ., USA; [6]Molecular Foundry,, Lawrence Berkeley National Laboratory, USA; [7]Stanford Synchrotron Radiation Laboratory, Stanford Univ. , USA; [8]Materials and Manufacturing Directorate, Air Force Research Laboratory, USA.* We analyze strain and corrugation derived upon growth and transferred mechanisms to foreign substrates of graphene at wafer scale by a combination of first-principles simulations and measurements of angle-resolved hyperspectral x-ray absorption spectroscopy.

Features of narrow-band ASE noise pulsing

Y. O. Barmenkov[1], P. Muniz-Cánovas[1], A. V. Kir'yanov[1], J. L. Cruz[2], and M. V. Andrés[2]
[1]*Centro de Investigaciones en Optica, Loma del Bosque 115, 37150, Leon, Mexico*
[2]*Departamento de Fisica Aplicada, Instituto de Ciencia de Materiales, Universidad de Valencia, 46100 Valencia, Spain*
Author e-mail address: yuri@cio.mx

Abstract: The results of an experimental study of noise features of polarized and unpolarized amplified spontaneous emission (ASE) with narrow optical bandwidth, registered from standard low-doped erbium fiber pumped at 976 nm, are presented.
OCIS codes: (060.2410) Fibers, erbium; (060.4370) Nonlinear optics, fibers; (270.5290) Photon statistics.

1. Introduction

Light sources based on amplified spontaneous emission (ASE) are characterized by a broad optical spectrum and high temporal stability due to the absence of relaxation oscillations and interference effects. It is known that ASE photon noise is described by M-fold degenerate Bose-Einstein distribution, where M relates to number of independent ASE states (modes) [1,2] and defined by ratio ξ of ASE optical spectrum width, B_{opt}, to photodetector electric bandwidth, B_{el}, and number of independent polarization states, s.

In this work, the experimental data on random ASE noise pulsing at ~ 1.55 μm arising in an erbium-doped fiber amplifier (EDFA) is presented; to assess a statistical analysis, ASE signal was optically filtered by means of a set of fiber Bragg gratings (FBGs) with different spectral widths, ranging from 20 pm to 230 pm.

In is shown that ASE noise is composed of train of Gaussian-like pulses with randomly varied magnitudes, widths, and sequencing intervals; distributions of these parameters are obtained and analyzed. It is also shown that the distribution of time derivative of ASE signal defines triangularity of optical spectrum broadening (when presented in semi-logarithmic scale), resulting from self-phase modulation in optical fiber.

This study serves for deeper understanding the ASE noise phenomena and addressing the specific nonlinear effects in optical fibers when ASE noise is used as pump.

2. Experimental results

The experimental setup is shown in Fig. 1(a). It contains two EDFAs based on standard low-doped EDF (EDF1 and EDF2) pumped at 976 nm through wavelength divisional multiplexers (WDM1 and WDM2). FBG1 and FBG2 partially reflect ASE signal of relatively broad optical spectrum (~ 600 pm) and FBG3 serves as a narrow-band band-pass filter.

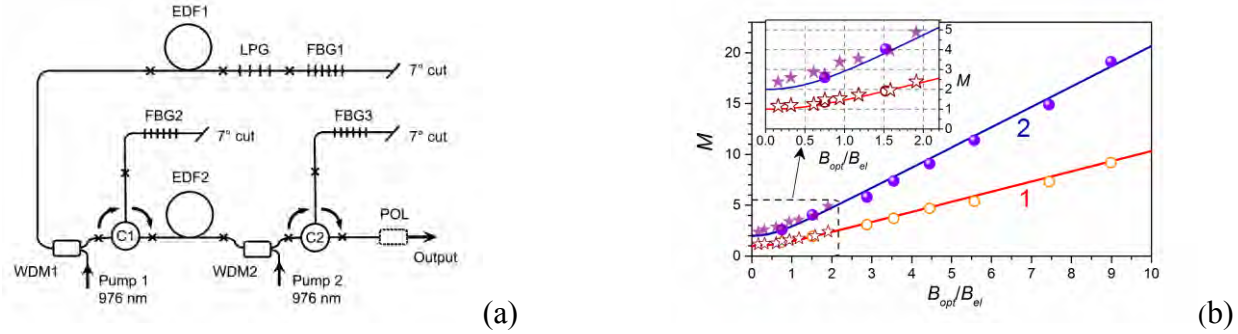

Fig. 1. (a) Experimental setup; C1 and C2 are fiber circulators and POL is fiber polarizer used for studying properties of polarized ASE (s = 1); long-period grating (LPG) centered at 1530 nm protects the first EDFA against parasitic lasing at this wavelength. (b) Mode number M *vs.* ξ, obtained for different ASE spectra using photo-receiving circuits with 15.5 GHz (stars) and 3.2 GHz (circles) RF bands; curves 1 and 2 correspond to polarized (s=1) and unpolarized (s=2) ASE, respectively.

The measured mode number M in function of $\xi=B_{opt}/B_{el}$ is plotted in Fig. 1(b) where the experimental points were obtained by analyzing the histograms of the photon count distributions (see e.g. Ref. [3]). It is seen that the experimental dependencies are well fitted by the theoretical curves (solid lines), obtained using Eq. 6.1-20 from Ref. [1], see also Ref. [2]; this reveals thermal nature of photon noise from the ASE source under study.

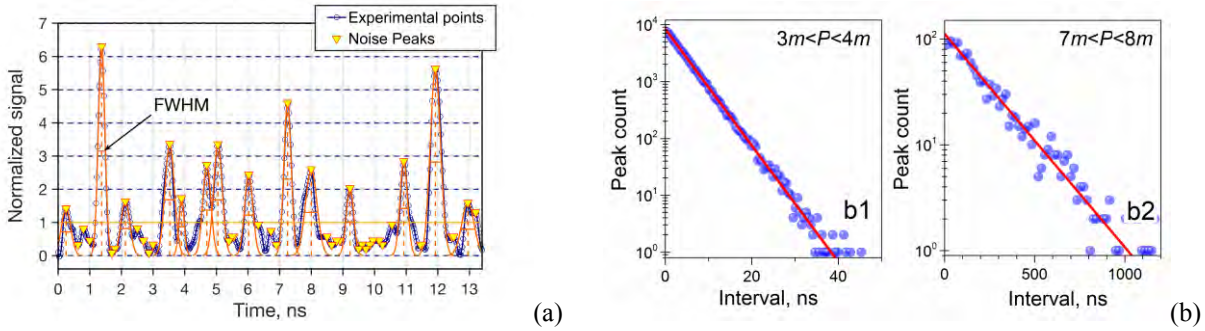

Fig. 2. (a) Example of a short scan of ASE photon noise obtained for $\xi << 1$ and $s = 1$; the noise signal is normalized to the mean value. Circles are experimental points and solid lines are Gaussian fits. (b) Examples of the peak count distributions (the peaks are shown in (a) by triangles) *vs.* the pulse sequence intervals for two ranges of peaks' magnitudes P; m means the ASE mean value.

It is seen from Fig. 2(a), exemplifying ASE detected with an oscilloscope, that ASE photon noise consists of train of Gaussian-like pulses with random magnitudes, widths, and inter-pulse intervals. We found that the noise peaks' distribution adheres to the ideal Bose-Einstein distribution with $M = 1$ and 2, for polarized and unpolarized ASE, respectively. Furthermore, from Fig. 2(b), one sees that probability of the shorter intervals between sequencing noise peaks of the same range of magnitudes P is higher (see the vertical axes) than that of the longer intervals. It is also seen that probability of ASE peaks decays exponentially with increasing interval between the peaks, slower for the more intense peaks than for the ones of lower magnitude (compare X-scaling in panels (b1) and (b2)).

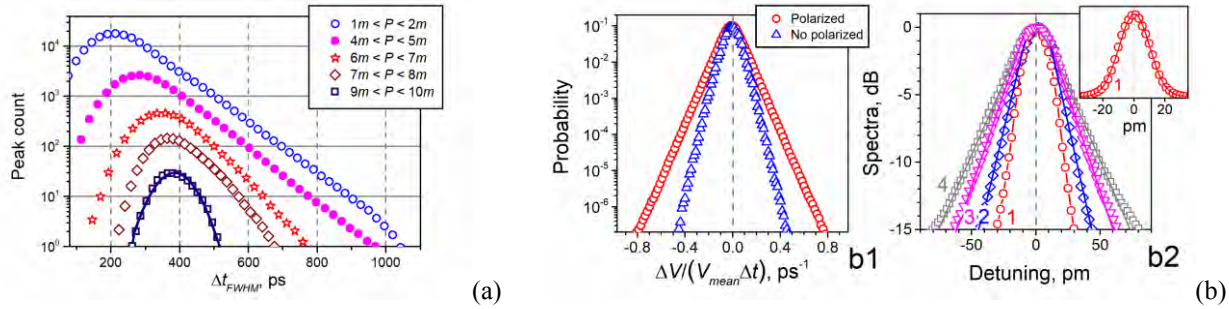

Fig. 3. (a) Distribution of widths (FWHM) of ASE peaks for $\xi << 1$and $s = 1$. (b) Distribution of normalized derivative of ASE noise (b1) and experimental broadening of ASE spectrum at the output of a long communication fiber (b2). Curve 1 shows the original ASE spectrum (inset demonstrates the spectrum in linear scale, the solid line is Gaussian fit) and curves 2, 3, and 4 exemplify the output spectra for different input ASE powers: 30, 52, and 82 mW, respectively.

Fig. 3(a) demonstrates the distribution of ASE pulse width (FWHM) for different magnitudes of the pulses. It is seen that the smaller noise peaks are narrower and the larger ones are wider, with the most probabilistic ones being ~200 and 400 ps, respectively; moreover, the FWHM distributions for the smaller peaks are broader and strongly asymmetrical (see the upper curves) while those for the bigger ones are narrower and more symmetrical (see the lowest curve, fitted by Gaussian function – solid line). Hence, the bigger in magnitude pulses are more stable in width as compared to the smaller ones.

From Fig. 3(b1), it is seen that probability of ASE signal's derivative is triangular in semi-logarithmic scale. Expectedly, the shape of ASE spectral broadening results from self-phase modulation (SPM), also triangular when presented in the same scale. This has been confirmed experimentally, see Fig. 3(b2) where we demonstrate the normalized spectra of narrow-band ASE measured on the input of 20 km-communication fiber (curve 1) and those on its output (curves 2 to 4). As seen, SPM-broadening is almost triangular, with slight deviation from this shape observed below -13 dB level at maximal ASE power (82 mW), stemming from two small rudimental peaks (not shown here) inherent to modulation instability.

References

[1] J. W. Goodman, *Statistical Optics* (Wiley, NY, 2000).

[2] S. M. Pietralunga *et al*., "Photon statistics of amplified spontaneous emission in a dense wavelength-division multiplexing regime," Opt. Lett. **28**, 152-154 (2003).

[3] J. A. Minguela-Gallardo *et al*., "Photon statistics of actively Q-switched erbium-doped fiber laser," JOSA B **34,** 1407-1414 (2017).